Published for SISSA by Springer

Received: June 4, 2012
Revised: July 27, 2012
Accepted: August 4, 2012
Published: August 28, 2012

Top-mass effects in differential Higgs production through gluon fusion at $\mathcal{O}(\alpha_s^4)$

Robert V. Harlander,[a] **Tobias Neumann,**[a] **Kemal J. Ozeren**[b] **and Marius Wiesemann**[a,c]

[a] *Fachbereich C, Bergische Universität Wuppertal, 42097 Wuppertal, Germany*

[b] *Department of Physics and Astronomy, UCLA, Los Angeles, CA 90095-1547, U.S.A.*

[c] *TH Division, Physics Department, CERN, CH-1211 Geneva 23, Switzerland*

E-mail: harlander@physik.uni-wuppertal.de, tobias.neumann@uni-wuppertal.de, marius.wiesemann@cern.ch, ozeren@physics.ucla.edu

Abstract: Effects from a finite top quark mass on differential distributions in the Higgs+jet production cross section through gluon fusion are studied at next-to-leading order in the strong coupling, i.e. $\mathcal{O}(\alpha_s^4)$. Terms formally subleading in $1/m_t$ are calculated, and their influence on the transverse momentum and rapidity distribution of the Higgs boson are evaluated. We find that, for the differential K-factor, the heavy-top limit is valid at the 2–3% level as long as the transverse momentum of the Higgs remains below about 150 GeV.

Keywords: NLO Computations, Hadronic Colliders

ArXiv ePrint: 1206.0157

doi:10.1007/JHEP08(2012)139

JHEP08(2012)139

Contents

JHEP08(2012)139

1 Introduction

The past few years in particle physics have been characterized by ever more sensitive exclusion limits for Higgs bosons (see, e.g., refs. [1–3]). These results were based on the combination of experimental data, background calculations and extrapolations, theoretical expectations for the signal, and careful estimates of the associated uncertainties [4, 5]. Concerning the signal cross sections, these uncertainties have several sources: the parton densities (PDFs), the strong coupling $\alpha_s(M_Z)$, and higher order perturbative effects, for example.

An uncertainty which is very specific to hadronic Higgs production in the Standard Model concerns the error induced by evaluating higher order perturbative corrections in an effective theory, derived by letting $m_t \to \infty$, where m_t is the top quark mass. The observation that the next-to-leading order (NLO) corrections to the inclusive total cross section are approximated at the percent level [6, 7] in this approach has been used as an argument for trusting it also at higher orders: next-to-NLO (NNLO) QCD corrections [8–10] have thus led to a perturbatively robust prediction for this quantity.[1] A few years ago, the effective theory approach was tested at NNLO by an explicit calculation of the subleading terms in $1/m_t$ to the total inclusive cross section [20–23]. It was found that these terms have an effect of less than 1%.

However, this result does not allow for a direct generalization to less inclusive quantities. Since they depend on several kinematical parameters such as the transverse momentum p_{T}, the rapidity y, or simply phase space cuts, such observables may have a very different convergence behavior in $1/m_t$ than the inclusive cross section.

[1] Effects beyond NNLO and electro-weak corrections have been studied in refs. [11–19], for example.

Nevertheless, so far the NLO p_T- and y-distributions in H+jet-production [24–27], the jet-vetoed Higgs cross section [28], as well as the resummation of the logarithmic terms for small p_T [29–32] are based on the effective theory approach, of course, and so are the fully exclusive NNLO partonic Monte Carlo programs for Higgs production in gluon fusion [33–35].

Only rather few studies have been aimed at quantitatively testing or going beyond the heavy-top approximation in Higgs distributions. Such results are only available at leading order (LO) in perturbation theory, for $H+n$jet with $n = 0, 1, 2$ [36–40]. Generally speaking, one finds that the approximation works rather well for $p_T < m_t$.

In this paper, we evaluate the $1/m_t$-effects to H+jet production at NLO QCD. We focus on the initial states gg and qg which, in the $\overline{\text{MS}}$ scheme, are typically about two orders of magnitude larger than all other channels combined. We will show that the radiative corrections to the mass effects in the gg channel are remarkably close to those of the heavy-top limit. In the sum over all partonic sub-processes, this is deteriorated to some extent by the qg-channel which is numerically subleading, however. As a result, we find that the kinematical distributions can be calculated with 2-3% accuracy by reweighting the LO distributions (including the full top mass dependence) by the differential NLO K-factor evaluated in the heavy-top mass limit.

A related uncertainty on the gluon fusion cross section arises due to the bottom-quark mediated gluon-Higgs coupling. Since the heavy-quark approximation is not applicable in this case, the calculation of higher order effects is much more complicated. They are in general available only one order lower in α_s than for the top quark contributions. However, due to the small bottom Yukawa coupling, these effects are parametrically suppressed: In the total cross section, they amount to about 7% for $m_H = 125\,\text{GeV}$ at NLO, with decreasing influence towards higher Higgs masses (see, e.g., ref. [6]). Their impact on distributions can be significantly larger though, reaching up to 20%, in particular when matched to parton showers [39, 40]. In this paper, we are not aiming at a comprehensive error estimate of the cross section which would have to include these effects, of course. Rather, we focus on the particular aspect of a finite top quark mass.

The remainder of the paper is organized as follows: In section 2, we briefly specify the problem under consideration by introducing the relevant Feynman diagrams; section 3 presents some LO motivation of our study; section 4 contains the main part of the paper, including the results for the p_T-integrated cross section as well as for the p_T and rapidity distributions, all at NLO; our conclusions are given in section 5.

2 Outline of the problem

In this paper we consider the quantities $\mathrm{d}\sigma/\mathrm{d}p_T$ and $\mathrm{d}\sigma/\mathrm{d}y$ in the gluon fusion process, where a Higgs boson is produced in association with a jet in hadronic collisions through a top-loop mediated gluon-Higgs coupling. Other quark-loop contributions are suppressed by their Yukawa coupling and will be neglected. The Higgs' transverse momentum p_T and its rapidity y are measured relative to the hadronic center-of-mass system. The LO contribution to this process is of order α_s^3; it is obtained by convolving the partonic subprocesses

JHEP08(2012)139

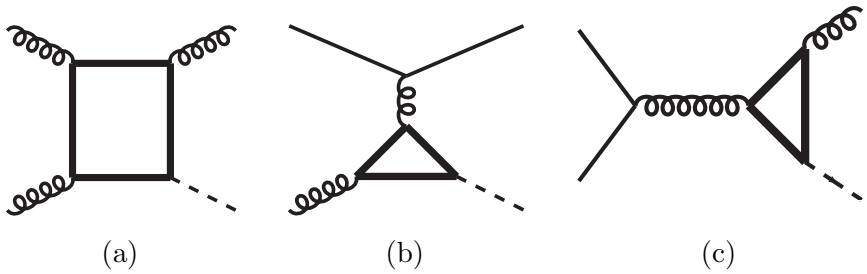

Figure 1. Sample Feynman diagrams contributing to the process $pp \to H$+jet at LO QCD. The graphical notation for the lines is: thick straight $\hat{=}$ top quark; thin straight $\hat{=}$ light quark $q \in \{u, d, c, s, b\}$; spiraled $\hat{=}$ gluon; dashed $\hat{=}$ Higgs boson.

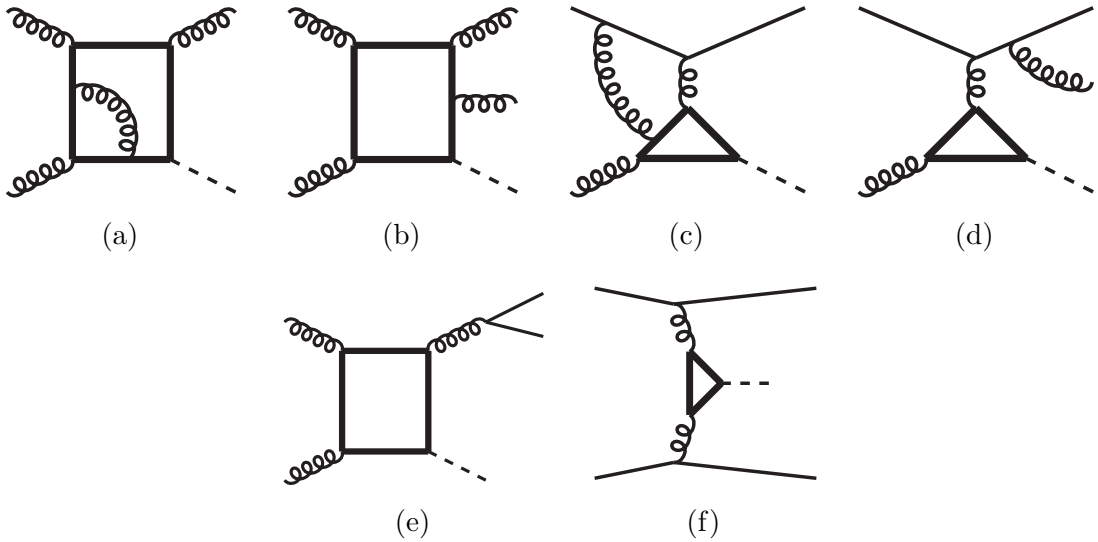

Figure 2. Sample Feynman diagrams contributing to the process $pp \to H$+jet at NLO QCD. Notation as in figure 1.

$gg \to Hg$, $qg \to Hq$, $\bar{q}g \to H + \bar{q}$, and $q\bar{q} \to Hg$ ($q \in \{u, d, s, c, b\}$), see figure 1, with the corresponding parton density functions. At this order of perturbation theory, the full dependence on the top quark and Higgs boson mass m_H is known, and also parton shower effects have been evaluated [39, 40].

At NLO, the Feynman diagrams can be divided into three groups: the first one is obtained by dressing each of the partonic LO processes by a virtual or a real gluon, see figure 2 (a)-(d), for example; the second one by splitting the emitted gluon into a $q\bar{q}$-pair, see figure 2 (e). The third group is of the form $q_1 q_2 \to H q_1 q_2$, where both q_1 and q_2 run continuously from the inital to the final state, and q_1, q_2 denote quarks or anti-quarks of the first five flavors, see figure 2 (f), for example.

3 Leading order considerations

Figure 3 shows the LO result for the cross section

$$\sigma(p_{\mathrm{T}} > p_{\mathrm{T}}^{\mathrm{cut}}) = \int_{p_{\mathrm{T}} \geq p_{\mathrm{T}}^{\mathrm{cut}}} \mathrm{d}p_{\mathrm{T}} \, \frac{\mathrm{d}\sigma}{\mathrm{d}p_{\mathrm{T}}} \tag{3.1}$$

JHEP08(2012)139

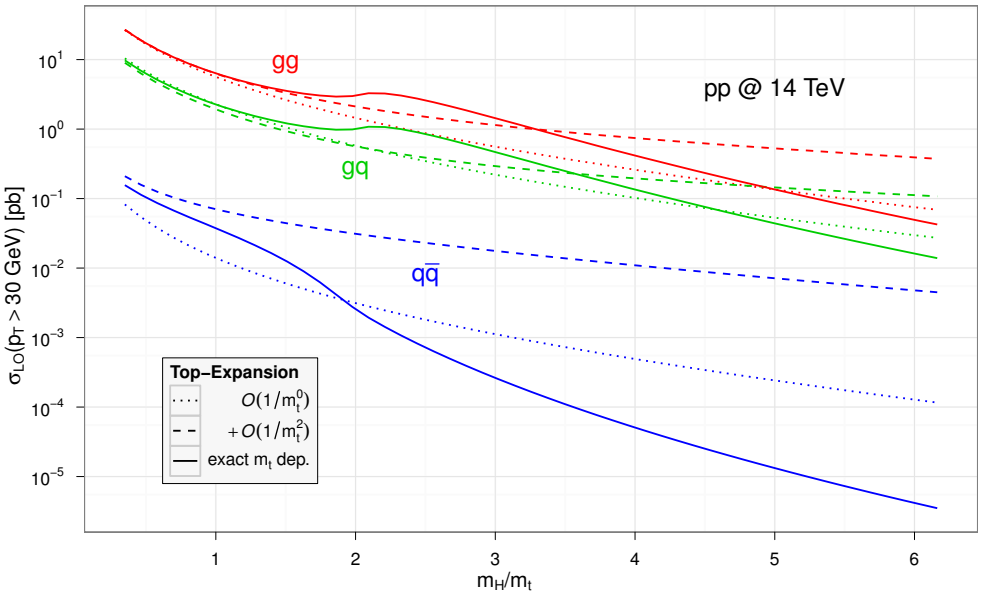

Figure 3. Higgs+jet cross section as defined in eq. (3.1), with $p_{\mathrm{T}}^{\mathrm{cut}} = 30\,\mathrm{GeV}$.

as a function of m_H, divided into the individual partonic sub-processes according to the $\overline{\mathrm{MS}}$-scheme, and keeping the full top mass dependence (solid), the expansion in $1/m_t$ through $1/m_t^0$ (dotted), and through $1/m_t^2$ (dashed). Unless stated otherwise, we will set $p_{\mathrm{T}}^{\mathrm{cut}} = 30\,\mathrm{GeV}$ in this paper; also, we choose the renormalization and factorization scales to be $\mu_{\mathrm{R}} = \mu_{\mathrm{F}} = m_H$; the on-shell top quark mass is set to $m_t = 172\,\mathrm{GeV}$, and the default hadronic center-of-mass energy is $\sqrt{s} = 14\,\mathrm{TeV}$, but we will include exemplary results for $\sqrt{s} = 7\,\mathrm{TeV}$ below.

The kink in the cross section at $m_H \approx 2m_t$ in figure 3 is due to the top-quark threshold in the scattering amplitude. Clearly, this structure cannot be reproduced by an expansion in $1/m_t$. Note that the shape of the curve is very reminiscent of the total inclusive cross section $pp \to H + X$ through gluon fusion which, however, is a $2 \to 1$ process at LO and starts at $\mathcal{O}(\alpha_s^2)$; the quantity displayed here is the cross section for H+jet production and therefore of $\mathcal{O}(\alpha_s^3)$.

As is obvious from figure 3, the $1/m_t$-expansion for the $q\bar{q}$ channel is significantly worse than for the other two channels. This failure of the $1/m_t$-expansion to reproduce the $q\bar{q}$-channel has already been observed for the total inclusive cross section in refs. [21, 23]. However, the $q\bar{q}$-channel is about two orders of magnitude smaller than qg which itself is a factor of 2-3 smaller than gg. Similar observations hold for the other purely quark induced channels which enter at higher orders, specifically qq, qq', and $q\bar{q}'$. The conclusion to draw from this is that the quark-induced channels constitute a solid, but rather minor limitation of the heavy-top limit. Our analysis cannot bring any further insights for these channels, and we will disregard them in what follows. One should keep in mind, however, that kinematical cuts could enhance the pure quark channels; in this case, results based on the heavy-top limit become unreliable.

JHEP08(2012)139

The relative deviation of the $1/m_t$-expansion from the exact result (still at LO) is shown in figure 4 (a). The curves are obtained by dividing the integrated cross section as defined in eq. (3.1) when expanded in $1/m_t$ by the same expression when the full top mass dependence is kept. The individual plots show this ratio separately for the case when only the gg-channel (left) and only the qg-channel (center) is taken into account (both in the numerator and the denominator of the ratio), and also for the sum of both channels (right). At this point, despite our default choice for the center-of-mass energy of $\sqrt{s} = 14\,\text{TeV}$, we also include results for $\sqrt{s} = 7\,\text{TeV}$ in order to obtain an impression of the dependence of our results on $\sqrt{s}$. The corresponding plots are shown in figure 4 (b). In the following discussion, the numbers for $\sqrt{s} = 7\,\text{TeV}$ are referred to in brackets; the unbracketed numbers are for the default $\sqrt{s} = 14\,\text{TeV}$.

For the gg-channel, the heavy-top expansion through $\mathcal{O}(1/m_t^2)$ approximates the exact result up to 2% (2.5% for $\sqrt{s} = 7\,\text{TeV}$) within $m_H \in [100, 200]\,\text{GeV}$, while the leading $\mathcal{O}(1/m_t^0)$ term deviates up to 15% (16%) from it. For the qg-channel, the approximation by the $1/m_t^2$-result is not as good: while the $1/m_t^0$-term remains within about 7% (5%) of the exact result, the $1/m_t^2$-term deviates by up to 18% (9.5%). However, since the gg-channel is numerically dominant, for the sum of both channels the $1/m_t^2$-approximation agrees with the full result to better than 6% (5%), while the difference between the $1/m_t^0$- and the exact result ranges up to 12% (12.5%).

We see that the dependence of the $1/m_t$-effects on the center-of-mass energy is very weak for the dominant gg-channel; for the qg-channel, the $1/m_t$-effects are more pronounced for higher $\sqrt{s}$ due to the fact that, technically, m_t is always assumed to be the largest scale in the problem (for a more detailed discussion, see ref. [20, 22, 41, 42]). In order to study the quality of the heavy-top approximation, it is therefore sufficient to use our default setting $\sqrt{s} = 14\,\text{TeV}$.

The absolute size of the mass effects at LO is used here only as an indicator of how far we can expect to be able to trust the heavy-top expansion at NLO. This indicator can be considered as a lower limit for the validity range though: In the total inclusive cross section, it has proved useful to factor out the LO top mass dependence from the perturbative corrections. Our results will show that it is very advantageous to follow this strategy also for differential cross sections.

Turning to more exclusive quantities, figure 5 compares the exact result for the Higgs' transverse momentum distribution to expansions including successively higher orders in $1/m_t$, separately for the gg- and the qg-channel. The $1/m_t$-expansion works very well, roughly up to $p_\text{T} = m_t$, as long as one restricts oneself to lower orders in $1/m_t$. At $\mathcal{O}(1/m_t^6)$ and beyond, convergence seems to be lost at much lower values of p_T. This is due to the region of large partonic center-of-mass energy $\sqrt{\hat{s}}$: similar to the calculation of ref. [20–23], the $1/m_t$-expansion generates a power behavior in $\hat{s}/m_t^2$. At lower orders in $1/m_t$, these terms are suppressed by the parton densities. At higher orders, however, they spoil the convergence behavior of the hadronic cross section. In our NLO analysis, we therefore restrict ourselves to comparisons of the $1/m_t^0$- to the $1/m_t^2$-terms.

The behavior of $\mathrm{d}\sigma/\mathrm{d}p_\text{T}$ suggests to try to improve the approximation of the integrated cross section $\sigma(p_\text{T} > p_\text{T}^\text{cut})$ by discarding the $1/m_t^2$-effects above $p_\text{T} \gtrsim 150\,\text{GeV}$, and taking

JHEP08(2012)139

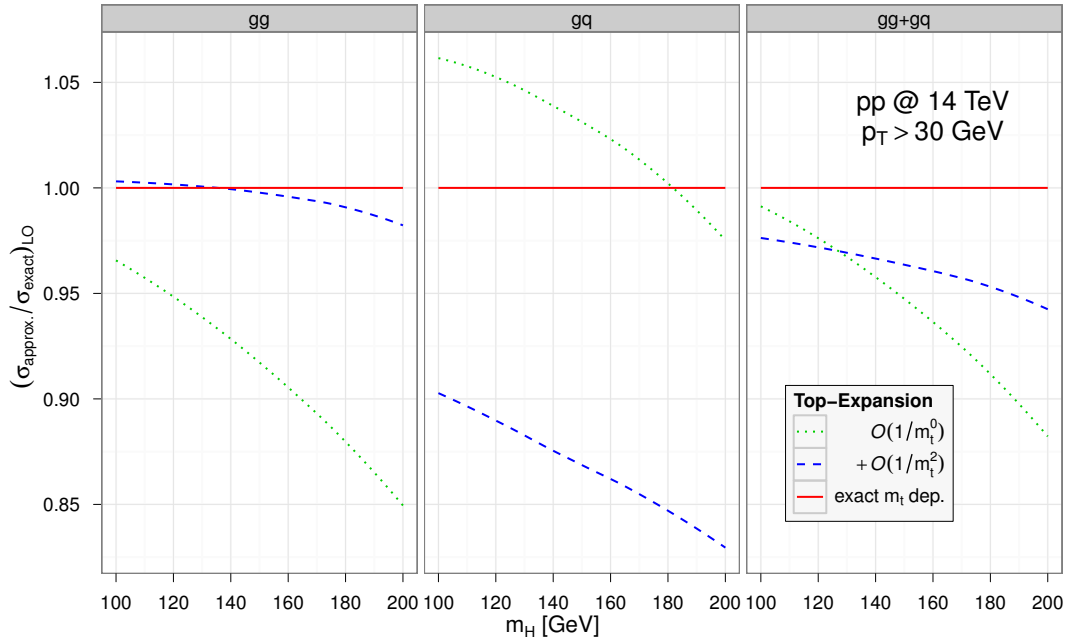

(a)

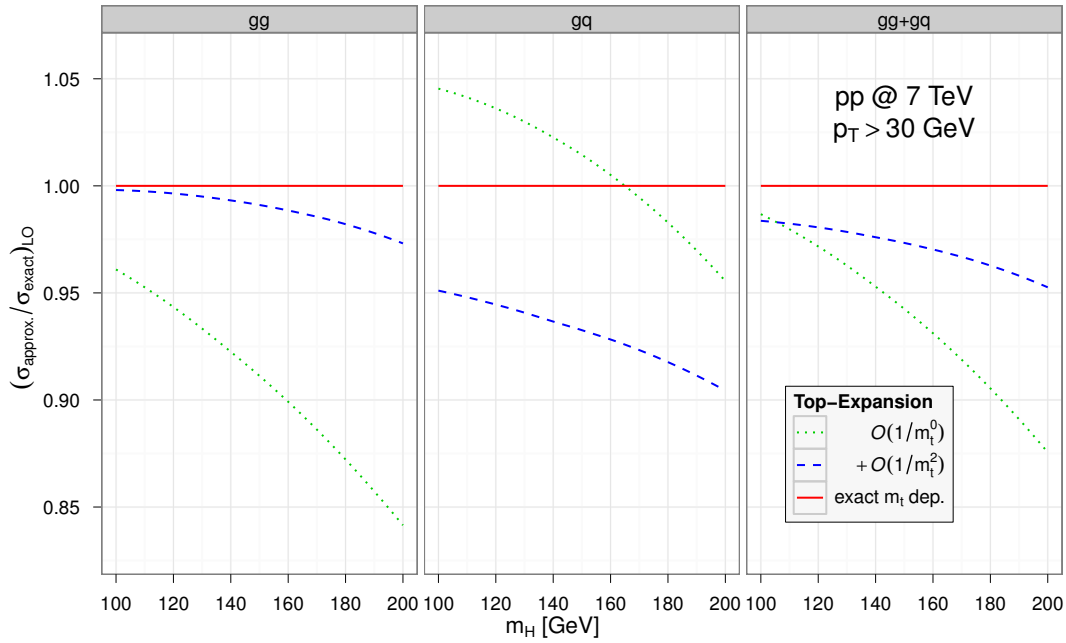

(b)

Figure 4. Ratio of the integrated LO cross section from eq. (3.1) when expanded through $1/m_t^n$ to the exact result, for $n = 0$ (dotted) and $n = 2$ (dashed). Left: only gg; center: only qg; right: sum of gg and qg; (a) $\sqrt{s} = 14\,\text{TeV}$ — (b) $\sqrt{s} = 7\,\text{TeV}$.

JHEP08(2012)139

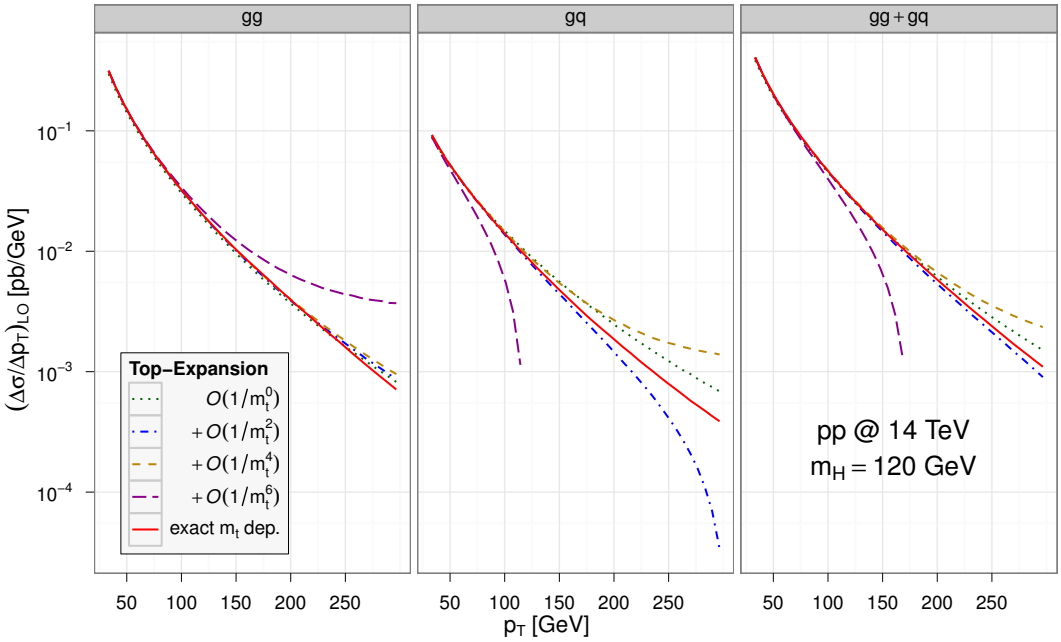

Figure 5. Differential cross section $d\sigma/dp_T$ at LO QCD, where p_T is the transverse momentum of the Higgs boson. Solid curve: full m_t-dependence included; dotted/dash-dotted/short-dashed/long-dashed: expansion in $1/m_t^n$ with $n = 0/2/4/6$. Left, center, and right plot show the gg-, the qg-channel, and their sum, respectively.

into account only the leading $1/m_t^0$ terms for larger values of p_T. The result is shown in figure 6. While the effect of this procedure is small in the gg-channel, the contribution from $p_T > 150\,\text{GeV}$ is much more significant in the qg-channel. Even though the numerical approximation improves, in particular for the sum $gg + qg$, this rather large effect indicates that the result depends quite strongly on the specific upper cut on p_T which has been introduced for the $1/m_t^2$ terms. We conclude that this does not allow for a systematic improvement and will not consider it any further.

Overall, the LO observations are encouraging to study the behavior of the $1/m_t$-terms at NLO in order to estimate the validity range of the heavy-top limit also for differential quantities.

4 Next-to-leading order results

4.1 Outline of the calculation

The most complicated Feynman diagrams are of the two-loop box-type with massless and massive (mass m_t) internal and one massive external line (mass m_H), see figures 2 (a) and (c), for example. Although not out of reach, the complexity of the corresponding integrals is too high for an efficient numerical evaluation. Therefore, to date the NLO corrections to this process are only available in an effective theory approach where the top quark is integrated out [24–27]. The Feynman diagrams then simplify to one-loop level, with an

JHEP08(2012)139

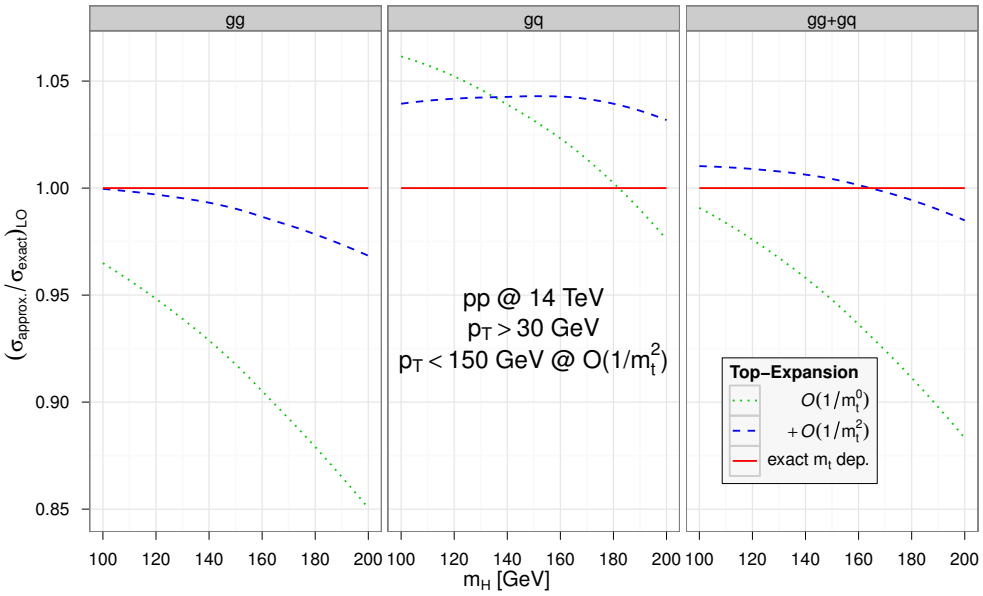

Figure 6. Similar to figure 4, but with an upper p_T-cut for the $1/m_t^2$-coefficient: $1/m_t^2 \to 1/m_t^2 \cdot \Theta(150 - p_{T/}\text{GeV})$.

effective Higgs-gluon vertex, multiplied by a Wilson coefficient which can be evaluated perturbatively [43–47].

The effective theory approach can be seen as the leading term of an expansion for small $1/m_t$. The goal of this paper is to go beyond this limit and to study the behavior of the next term in this expansion. In ref. [20], the relevant one-loop $2 \to 2$ and tree-level $2 \to 3$ amplitudes have been obtained through automated asymptotic expansions [48–50]. For our purposes, we combine them here with the dipole subtraction terms [51] which we have to take into account order by order in $1/m_t$, of course. The result is a NLO Monte Carlo program for H+parton production in gluon fusion which, in addition to the already available pure heavy-top limit [24–26], also includes the first formally subleading term in $1/m_t^2$.

We have performed a number of checks on our results. The two most important ones are the numerical comparison of the leading terms in $1/m_t$ with the non-resummed part of the program `HqT` [29, 30, 52] where we find agreement at the sub-percent level. The amplitudes for the $1/m_t^2$-terms have been checked previously by the agreement of the inclusive cross section between ref. [20] and [22]. Their proper implementation into a Monte Carlo program is checked by the independence of the numerical results on the so-called α-parameter [53, 54] which allows to restrict the phase space of the dipole terms.

4.2 Notation

We introduce the following notation for the individual terms in our expansions:

$$[\mathrm{d}\sigma_k^{(l)}]_{ij}^{\mathrm{X}}\,, \qquad \mathrm{X} \in \{\mathrm{LO}, \mathrm{NLO}\}\,, \qquad i,j \in \{q, \bar{q}, g\}\,, \tag{4.1}$$

JHEP08(2012)139

where l denotes the order of perturbation theory, k the order of the expansion in $1/m_t$, and X the order of the PDFs and the running of α_s that have been used.[2] The subscript ij denotes the particular partonic channel that was taken into account. If any of the indices l, k or ij are absent, it means that these indices are summed over all possible values. In addition, we define

$$\mathrm{d}\sigma^{\mathrm{LO}} \equiv [\mathrm{d}\sigma^{(0)}]^{\mathrm{LO}}\,, \quad \mathrm{d}\sigma^{\mathrm{NLO}} \equiv [\mathrm{d}\sigma^{(0)} + \mathrm{d}\sigma^{(1)}]^{\mathrm{NLO}}\,, \tag{4.2}$$

are the LO and the NLO differential cross sections with exact m_t-dependence, and summed over all parton channels (recall, however, that we neglect all $q\bar{q}$ and qq contributions in this paper).

In order to isolate the individual corrections to the cross section, we define the quantities

$$\begin{aligned}
[R_k^{(l)}(b)]_{ij} &= \frac{[\mathrm{d}\sigma_k^{(l)}(b)]_{ij}^{\mathrm{NLO}}}{\mathrm{d}\sigma^{\mathrm{LO}}(b)}\,, \\
[K_n(b)]_{ij} &= \frac{\sum_{k=0}^{n}[\mathrm{d}\sigma_k^{(0)}(b) + \mathrm{d}\sigma_k^{(1)}(b)]_{ij}^{\mathrm{NLO}}}{\sum_{k=0}^{n}[\mathrm{d}\sigma_k^{(0)}(b)]_{ij}^{\mathrm{LO}}}\,.
\end{aligned} \tag{4.3}$$

On the right hand side of these definitions, it is understood that $\mathrm{d}\sigma(b)$ is integrated over all kinematical variables *except* the set b, where we consider $b = \{p_{\mathrm{T}}\}$, $b = \{y\}$, and $b = \emptyset$ (i.e., transverse momentum and rapidity distributions, and the integrated cross section with $p_{\mathrm{T}} > 30\,\mathrm{GeV}$). Also, if ij is to be summed over, this applies separately to the numerator and the denominator in $[K_n(b)]_{ij}$. The ratio $R_k^{(l)}(b)$ allows for a direct comparison of the perturbative (index l) and the mass effects (index k). The quantity $K(b)$, on the other hand, shows the influence of the mass terms on the perturbative correction factor. For example, K_0 is the NLO K-factor in the heavy-top limit which — in the case of the total inclusive cross section — has been found to approximate the exact NLO K-factor extremely well. Using the $1/m_t$-expansion, we will study whether this observation can be expected to carry over also to differential quantities.

4.3 Inclusive Higgs plus jet production

The first observable we study is the integrated cross section for Higgs+jet production, defined in eq. (3.1). Figure 7 compares the NLO perturbative corrections to the mass effects at LO and at NLO, split into the two numerically dominant sub-channels gg (dotted) and qg (dashed), as well as for the sum of both channels (solid). The size of $R_0^{(0)}(\equiv R_0^{(0)}(\emptyset))$ is mostly determined by the reduced value of α_s when going from LO to NLO parton densities. $R_0^{(1)}$, on the other hand, reflects the well-known largeness of the perturbative effects to the gluon fusion cross section. Considering the fact that $R_0^{(1)}$ includes a factor α_s/π relative to $R_0^{(0)}$, it is remarkable that they are both almost equally large. Note also that both $R_0^{(0)}$ and $R_0^{(1)}$ depend only very weakly on the Higgs mass m_H.

[2] We use the central MSTW2008 PDF sets; related uncertainties are not the subject of this paper. See refs. [55, 56], however.

JHEP08(2012)139

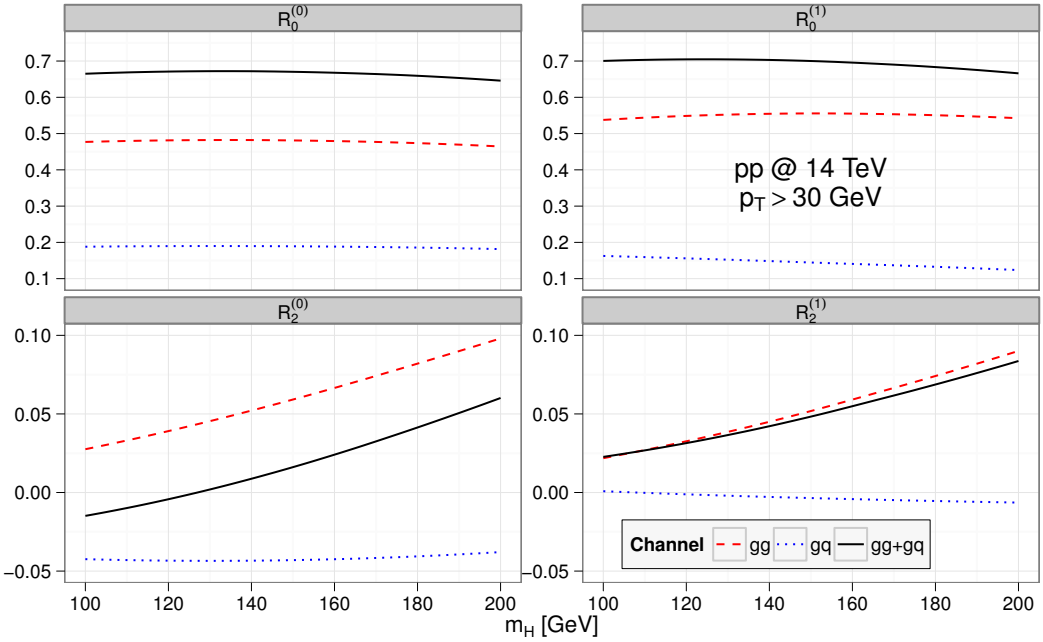

Figure 7. Relative size of the perturbative and the mass effects on the integrated cross section, $R_k^{(l)} \equiv R_k^{(l)}(\emptyset)$, see eq. (3.1) and eq. (4.3). Upper row: NLO effects arising solely from the PDFs and the running of α_s (left), and from the NLO perturbative coefficient in the cross section (right). Lower row: mass effects from the LO (left) and the NLO (right) perturbative coefficient. Dotted: only qg; dashed: only gg; solid: sum of gg and qg.

The same feature holds for the mass effects, shown in the lower two plots, separately for the LO (left) and the NLO (right) coefficients. Note also that there is a cancellation between the gg and the qg channels, although much less pronounced at NLO than at LO. The overall mass effects between $m_H = 100\,\text{GeV}$ and $200\,\text{GeV}$ range from -2% to 6% for the LO, and from 2% to 8% for the NLO coefficient. They are thus much smaller than the perturbative effects. As expected, the mass effects decrease for smaller Higgs masses.

Concerning the K-factor, for the total inclusive cross section it has been found to depend only very weakly on the top quark mass [6, 20, 22]. The product of the K-factor with the exact LO cross section is thus an excellent approximation of the higher order cross section.

Let us study the extent to which we can draw a similar conclusion for the cross section with a lower p_T cut. In figure 8, we compare the result for the K-factor including mass terms, K_2 ($\equiv K_2(\emptyset)$, cf. eq. (4.3)) to the pure heavy-top limit. Again, we consider separately the channels gg and qg, as well as their sum. Note however, that according to the definition in eq. (4.3), $[K_n]_{ij}$ really only refers to the ij channel, both in the numerator *and* the denominator. Therefore, $K_n \neq [K_n]_{gg} + [K_n]_{qg}$.

The agreement between K_0 and K_2 for the gg channel is truly remarkable; for the qg channel, we find 5-10% difference, but due to the numerical dominance of gg, the overall agreement between K_0 and K_2 is around 3%.

JHEP08(2012)139

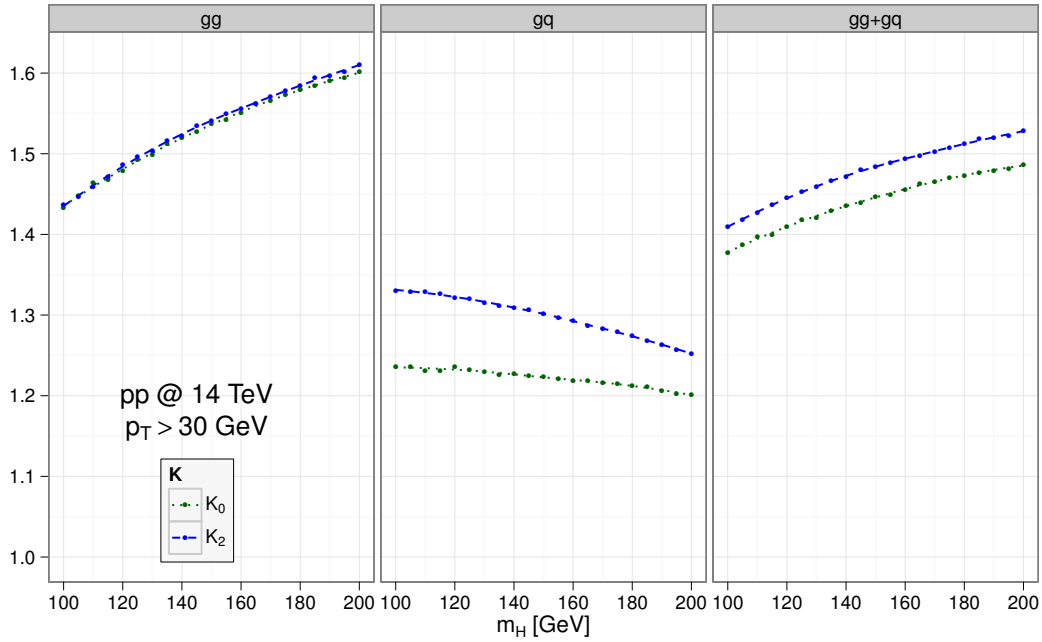

Figure 8. K-factors as defined in eq. (4.3), for the integrated cross section, i.e. $K_n \equiv K_n(\emptyset)$. Left/center/right plot: $[K_n]_{gg}/[K_n]_{qg}/[K_n]_{gg+qg}$. Dotted/dashed: $n = 0/2$. The dots show the results of our calculation; the lines have been introduced to guide the eye. The deviation between the dots and the lines indicates our numerical error.

4.4 Transverse momentum distribution

Figure 9 shows the p_T-dependent ratio $R(p_T)$ ($\equiv R(\{p_T\})$, cf. eq. (4.3)), in analogy to figure 7. The qualitative features of the individual corrections for this differential quantity are very similar to the integrated ones. An observation that deserves to be pointed out is the stunning similarity of the plots for the mass effects at LO and NLO.

Both at LO and NLO, the mass terms in the gg-channel are very small ($\sim 2\%$) and almost independent of p_T, even up to $p_T = 300\,\text{GeV}$. The qg-channel behaves worse, but its mass terms still do not amount to more than 6% below $p_T = 150\,\text{GeV}$; at LO, they reach up to almost 50% at $p_T = 300\,\text{GeV}$ though. The NLO mass terms are only slightly smaller. The sum of gg and qg, however, remains below 35% at NLO for $p_T < 300\,\text{GeV}$; below $p_T = 150\,\text{GeV}$, they amount to not more than 3%. The mass effects reduce the absolute value of the cross section in the qg-channel significantly for $p_T > 150\,\text{GeV}$, which is also visible at LO in figure 5, while it just slightly affects the sum of both channels.

The p_T-dependent K-factors $K_n(p_T)$ ($\equiv K_n(\{p_T\})$) are shown in figure 10. The K-factors including leading and subleading mass terms, K_0 and K_2, are almost identical in the gg-channel. For the qg-channel, on the other hand, the QCD corrections to the subleading mass terms behave very differently to the leading terms in $1/m_t$ once $p_T > 150\,\text{GeV}$. In the sum of both channels, the difference remains below 3% for $p_T < 150\,\text{GeV}$, and reaches 10% at $p_T = 300\,\text{GeV}$.

JHEP08(2012)139

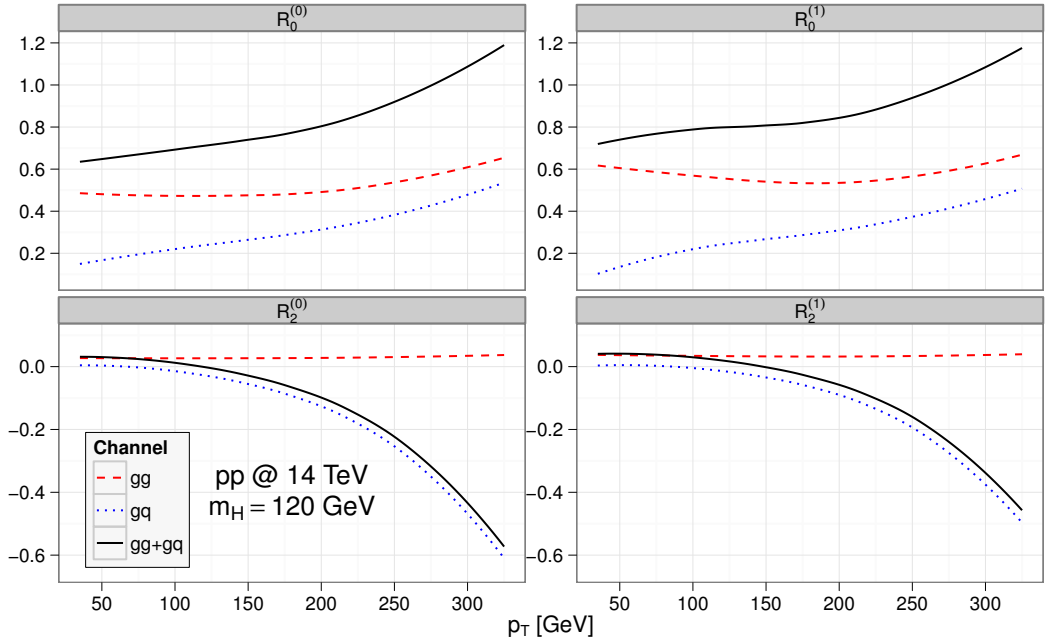

Figure 9. Similar to figure 7, but for the differential cross section $d\sigma/dp_T$; here, $R_k^{(l)} \equiv R_k^{(l)}(\{p_T\})$.

In conclusion, the behaviour of K_2 with respect to K_0 suggests that, also for the p_T-distribution, the QCD *corrections* can be safely calculated in the heavy-top limit; the accuracy remains within 2% (10%) below $p_T = 150\,\text{GeV}$ ($p_T = 300\,\text{GeV}$). The absolute distributions, however, should be calculated at LO using the full top-mass dependence, and then reweighted by these QCD corrections.

4.5 Rapidity distribution

Figure 11 shows the y-dependent ratios $R(y) \equiv R(\{y\})$. The perturbative effects, $R_0^{(0)}$ and $R_0^{(1)}$, are qualitatively very similar to the quantities discussed before. The mass effects are generally very small over the full y-range. At LO, there is a significant cancellation between the gg- and the qg- channel, so that the sum remains below 1% almost everywhere, even though the individual channels reach up to 4%. At NLO, the mass effects in the qg-channel are very small, but due to the numerical dominance of the purely gluon induced contributions, the overall effect reaches up to 4%.

The K-factors, shown in figure 12, display a similar behavior as in the previous observables: the corrections in the gg-channel are practically the same in the $1/m_t^0$- and the $1/m_t^2$-terms, the qg-channel shows some difference, but in the sum of both channels, the K_2 is approximated by K_0 to within about 3%. Apparently, the bad convergence of the qg-channel for $p_T > 150\,\text{GeV}$ as observed in section 4.4 affects p_T-integrated quantities only at the percent level, see also figure 8.

JHEP08(2012)139

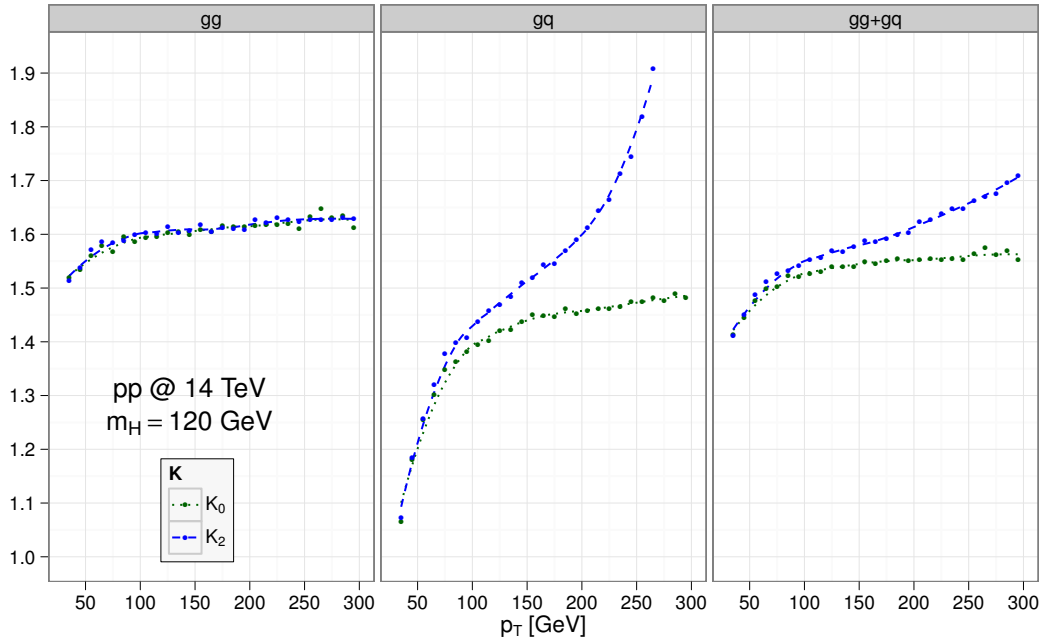

Figure 10. Similar to figure 8, but for the differential cross section $\mathrm{d}\sigma/\mathrm{d}p_{\mathrm{T}}$; here, $K_n \equiv K_n(\{p_{\mathrm{T}}\})$.

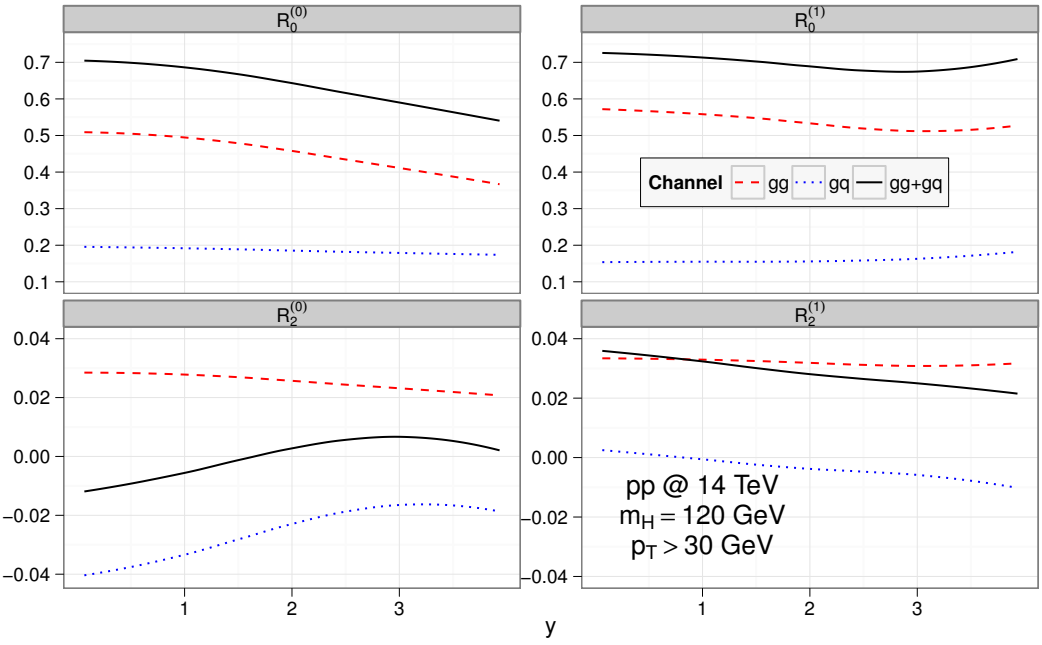

Figure 11. Similar to figure 7, but for the differential cross section $\mathrm{d}\sigma/\mathrm{d}y$; here, $R_k^{(l)} \equiv R_k^{(l)}(\{y\})$.

JHEP08(2012)139

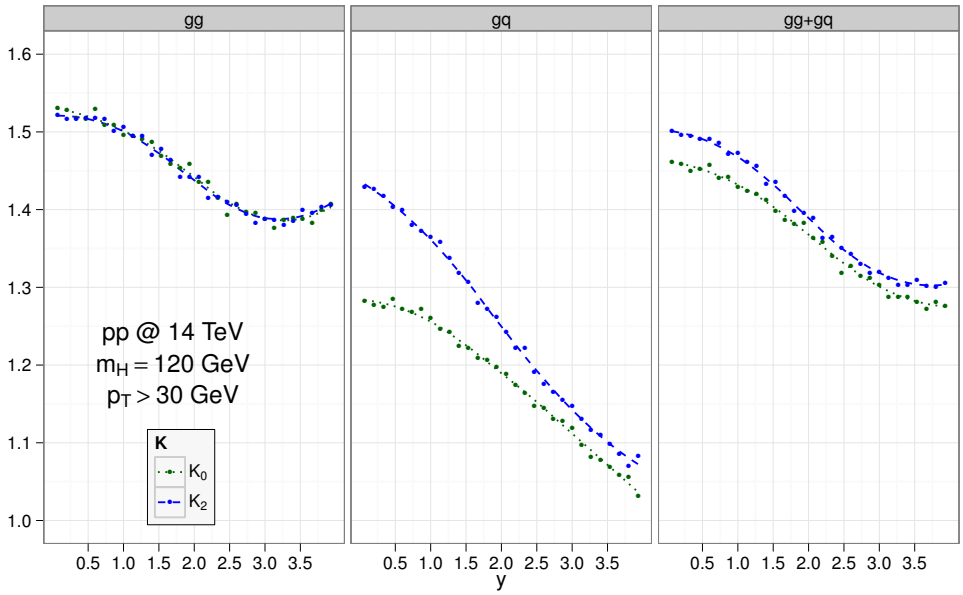

Figure 12. Similar to figure 8, but for the differential cross section $\mathrm{d}\sigma/\mathrm{d}y$; here, $K_n \equiv K_n(\{y\})$.

5 Conclusions

In this paper, the quality of the heavy-top limit in the gluon fusion cross section has been studied. Subleading terms in $1/m_t$ have been calculated for the H+jet cross section at NLO QCD, and their effects on the Higgs' transverse momentum and rapidity distribution have been evaluated.

We found that, similar to the leading terms in $1/m_t$, the perturbative corrections on the subleading terms are of order one. In fact, the perturbative effects on the mass corrections in the gg-channel are remarkably similar to those on the leading mass terms, both for the p_{T}- and the y-distribution, as well as for the integrated cross section of eq. (3.1). The NLO K-factors with and without mass terms are therefore almost identical for this channel alone. Including the qg-channel spoils this similarity to some extent, but we still claim that the procedure of correcting the full LO prediction (including top mass effect) by the K-factor as evaluated in the heavy-top limit provides an excellent approximation to the full NLO result, valid at the 2-3% level for $p_{\mathrm{T}} < 150\,\mathrm{GeV}$ and for p_{T}-integrated quantities. We have checked that this result holds for Higgs masses below $2m_t$. The accuracy is thus better than the current uncertainty on the cross section due to its dependence on the PDFs and due to missing higher order QCD corrections, including those from a bottom-quark mediated gluon-Higgs coupling.

Acknowledgments

This work was supported by BMBF contract 05H09PXE and LHCPhenoNet PITN-GA-2010-264564. The work of KO was supported by the US Department of Energy under contract DE-FG03-91ER40662.

JHEP08(2012)139

References

[1] TEVNPH, CDF, D0 collaboration, *Combined CDF and D0 search for standard model Higgs boson production with up to* $10.0\,fb^{-1}$ *of data*, arXiv:1203.3774 [INSPIRE].

[2] ATLAS collaboration, G. Aad et al., *Combined search for the standard model Higgs boson using up to* $4.9\ fb^{-1}$ *of pp collision data at* $\sqrt{s} = 7$ *TeV with the ATLAS detector at the LHC*, *Phys. Lett.* **B 710** (2012) 49 [arXiv:1202.1408] [INSPIRE].

[3] CMS collaboration, S. Chatrchyan et al., *Combined results of searches for the standard model Higgs boson in pp collisions at* $\sqrt{s} = 7$ *TeV*, *Phys. Lett.* **B 710** (2012) 26 [arXiv:1202.1488] [INSPIRE].

[4] LHC Higgs Cross Section Working Group collaboration, S. Dittmaier et al., *Handbook of LHC Higgs cross sections: 1. Inclusive observables*, arXiv:1101.0593 [INSPIRE].

[5] S. Dittmaier et al., *Handbook of LHC Higgs cross sections: 2. Differential distributions*, arXiv:1201.3084 [INSPIRE].

[6] M. Spira, A. Djouadi, D. Graudenz and P. Zerwas, *Higgs boson production at the LHC*, *Nucl. Phys.* **B 453** (1995) 17 [hep-ph/9504378] [INSPIRE].

[7] S. Dawson and R. Kauffman, *QCD corrections to Higgs boson production: nonleading terms in the heavy quark limit*, *Phys. Rev.* **D 49** (1994) 2298 [hep-ph/9310281] [INSPIRE].

[8] R.V. Harlander and W.B. Kilgore, *Next-to-next-to-leading order Higgs production at hadron colliders*, *Phys. Rev. Lett.* **88** (2002) 201801 [hep-ph/0201206] [INSPIRE].

[9] C. Anastasiou and K. Melnikov, *Higgs boson production at hadron colliders in NNLO QCD*, *Nucl. Phys.* **B 646** (2002) 220 [hep-ph/0207004] [INSPIRE].

[10] V. Ravindran, J. Smith and W.L. van Neerven, *NNLO corrections to the total cross-section for Higgs boson production in hadron hadron collisions*, *Nucl. Phys.* **B 665** (2003) 325 [hep-ph/0302135] [INSPIRE].

[11] S. Catani, D. de Florian, M. Grazzini and P. Nason, *Soft gluon resummation for Higgs boson production at hadron colliders*, *JHEP* **07** (2003) 028 [hep-ph/0306211] [INSPIRE].

[12] A. Idilbi, X.-d. Ji, J.-P. Ma and F. Yuan, *Threshold resummation for Higgs production in effective field theory*, *Phys. Rev.* **D 73** (2006) 077501 [hep-ph/0509294] [INSPIRE].

[13] V. Ravindran, *Higher-order threshold effects to inclusive processes in QCD*, *Nucl. Phys.* **B 752** (2006) 173 [hep-ph/0603041] [INSPIRE].

[14] V. Ahrens, T. Becher, M. Neubert and L.L. Yang, *Renormalization-group improved prediction for Higgs production at hadron colliders*, *Eur. Phys. J.* **C 62** (2009) 333 [arXiv:0809.4283] [INSPIRE].

[15] A. Djouadi and P. Gambino, *Leading electroweak correction to Higgs boson production at proton colliders*, *Phys. Rev. Lett.* **73** (1994) 2528 [hep-ph/9406432] [INSPIRE].

[16] G. Degrassi and F. Maltoni, *Two-loop electroweak corrections to Higgs production at hadron colliders*, *Phys. Lett.* **B 600** (2004) 255 [hep-ph/0407249] [INSPIRE].

[17] U. Aglietti, R. Bonciani, G. Degrassi and A. Vicini, *Two loop light fermion contribution to Higgs production and decays*, *Phys. Lett.* **B 595** (2004) 432 [hep-ph/0404071] [INSPIRE].

JHEP08(2012)139

[18] S. Actis, G. Passarino, C. Sturm and S. Uccirati, *NLO electroweak corrections to Higgs boson production at hadron colliders*, *Phys. Lett.* **B 670** (2008) 12 [arXiv:0809.1301] [INSPIRE].

[19] C. Anastasiou, R. Boughezal and F. Petriello, *Mixed QCD-electroweak corrections to Higgs boson production in gluon fusion*, *JHEP* **04** (2009) 003 [arXiv:0811.3458] [INSPIRE].

[20] R.V. Harlander and K.J. Ozeren, *Finite top mass effects for hadronic Higgs production at next-to-next-to-leading order*, *JHEP* **11** (2009) 088 [arXiv:0909.3420] [INSPIRE].

[21] R.V. Harlander, H. Mantler, S. Marzani and K.J. Ozeren, *Higgs production in gluon fusion at next-to-next-to-leading order QCD for finite top mass*, *Eur. Phys. J.* **C 66** (2010) 359 [arXiv:0912.2104] [INSPIRE].

[22] A. Pak, M. Rogal and M. Steinhauser, *Finite top quark mass effects in NNLO Higgs boson production at LHC*, *JHEP* **02** (2010) 025 [arXiv:0911.4662] [INSPIRE].

[23] A. Pak, M. Rogal and M. Steinhauser, *Production of scalar and pseudo-scalar Higgs bosons to next-to-next-to-leading order at hadron colliders*, *JHEP* **09** (2011) 088 [arXiv:1107.3391] [INSPIRE].

[24] D. de Florian, M. Grazzini and Z. Kunszt, *Higgs production with large transverse momentum in hadronic collisions at next-to-leading order*, *Phys. Rev. Lett.* **82** (1999) 5209 [hep-ph/9902483] [INSPIRE].

[25] C.J. Glosser and C.R. Schmidt, *Next-to-leading corrections to the Higgs boson transverse momentum spectrum in gluon fusion*, *JHEP* **12** (2002) 016 [hep-ph/0209248] [INSPIRE].

[26] V. Ravindran, J. Smith and W. Van Neerven, *Next-to-leading order QCD corrections to differential distributions of Higgs boson production in hadron hadron collisions*, *Nucl. Phys.* **B 634** (2002) 247 [hep-ph/0201114] [INSPIRE].

[27] D. de Florian, A. Kulesza and W. Vogelsang, *Threshold resummation for high-transverse-momentum Higgs production at the LHC*, *JHEP* **02** (2006) 047 [hep-ph/0511205] [INSPIRE].

[28] S. Catani, D. de Florian and M. Grazzini, *Direct Higgs production and jet veto at the Tevatron and the LHC in NNLO QCD*, *JHEP* **01** (2002) 015 [hep-ph/0111164] [INSPIRE].

[29] G. Bozzi, S. Catani, D. de Florian and M. Grazzini, *The q_T spectrum of the Higgs boson at the LHC in QCD perturbation theory*, *Phys. Lett.* **B 564** (2003) 65 [hep-ph/0302104] [INSPIRE].

[30] G. Bozzi, S. Catani, D. de Florian and M. Grazzini, *Transverse-momentum resummation and the spectrum of the Higgs boson at the LHC*, *Nucl. Phys.* **B 737** (2006) 73 [hep-ph/0508068] [INSPIRE].

[31] G. Bozzi, S. Catani, D. de Florian and M. Grazzini, *Higgs boson production at the LHC: transverse-momentum resummation and rapidity dependence*, *Nucl. Phys.* **B 791** (2008) 1 [arXiv:0705.3887] [INSPIRE].

[32] S. Catani and M. Grazzini, *QCD transverse-momentum resummation in gluon fusion processes*, *Nucl. Phys.* **B 845** (2011) 297 [arXiv:1011.3918] [INSPIRE].

[33] C. Anastasiou, K. Melnikov and F. Petriello, *Higgs boson production at hadron colliders: differential cross sections through next-to-next-to-leading order*, *Phys. Rev. Lett.* **93** (2004) 262002 [hep-ph/0409088] [INSPIRE].

[34] S. Catani and M. Grazzini, *HNNLO: a Monte Carlo program to compute Higgs boson production at hadron colliders*, PoS(RADCOR2007)046 [arXiv:0802.1410] [INSPIRE].

JHEP08(2012)139

[35] S. Catani and M. Grazzini, *An NNLO subtraction formalism in hadron collisions and its application to Higgs boson production at the LHC*, *Phys. Rev. Lett.* **98** (2007) 222002 [hep-ph/0703012] [INSPIRE].

[36] V. Del Duca, W. Kilgore, C. Oleari, C. Schmidt and D. Zeppenfeld, *Kinematical limits on Higgs boson production via gluon fusion in association with jets*, *Phys. Rev.* **D 67** (2003) 073003 [hep-ph/0301013] [INSPIRE].

[37] V. Del Duca, W. Kilgore, C. Oleari, C. Schmidt and D. Zeppenfeld, *Gluon fusion contributions to $H + 2$ jet production*, *Nucl. Phys.* **B 616** (2001) 367 [hep-ph/0108030] [INSPIRE].

[38] V. Del Duca, W. Kilgore, C. Oleari, C. Schmidt and D. Zeppenfeld, *Higgs +2 jets via gluon fusion*, *Phys. Rev. Lett.* **87** (2001) 122001 [hep-ph/0105129] [INSPIRE].

[39] J. Alwall, Q. Li and F. Maltoni, *Matched predictions for Higgs production via heavy-quark loops in the SM and beyond*, *Phys. Rev.* **D 85** (2012) 014031 [arXiv:1110.1728] [INSPIRE].

[40] E. Bagnaschi, G. Degrassi, P. Slavich and A. Vicini, *Higgs production via gluon fusion in the POWHEG approach in the SM and in the MSSM*, *JHEP* **02** (2012) 088 [arXiv:1111.2854] [INSPIRE].

[41] R.V. Harlander and K.J. Ozeren, *Top mass effects in Higgs production at next-to-next-to-leading order QCD: virtual corrections*, *Phys. Lett.* **B 679** (2009) 467 [arXiv:0907.2997] [INSPIRE].

[42] A. Pak, M. Rogal and M. Steinhauser, *Virtual three-loop corrections to Higgs boson production in gluon fusion for finite top quark mass*, *Phys. Lett.* **B 679** (2009) 473 [arXiv:0907.2998] [INSPIRE].

[43] K. Chetyrkin, B.A. Kniehl and M. Steinhauser, *Decoupling relations to $O(\alpha_s^3)$ and their connection to low-energy theorems*, *Nucl. Phys.* **B 510** (1998) 61 [hep-ph/9708255] [INSPIRE].

[44] M. Krämer, E. Laenen and M. Spira, *Soft gluon radiation in Higgs boson production at the LHC*, *Nucl. Phys.* **B 511** (1998) 523 [hep-ph/9611272] [INSPIRE].

[45] K. Chetyrkin, B.A. Kniehl and M. Steinhauser, *Hadronic Higgs decay to order α_s^4*, *Phys. Rev. Lett.* **79** (1997) 353 [hep-ph/9705240] [INSPIRE].

[46] Y. Schröder and M. Steinhauser, *Four-loop decoupling relations for the strong coupling*, *JHEP* **01** (2006) 051 [hep-ph/0512058] [INSPIRE].

[47] K. Chetyrkin, J.H. Kühn and C. Sturm, *QCD decoupling at four loops*, *Nucl. Phys.* **B 744** (2006) 121 [hep-ph/0512060] [INSPIRE].

[48] R. Harlander, T. Seidensticker and M. Steinhauser, *Complete corrections of order $\alpha\alpha_s$ to the decay of the Z boson into bottom quarks*, *Phys. Lett.* **B 426** (1998) 125 [hep-ph/9712228] [INSPIRE].

[49] M. Steinhauser, *MATAD: a program package for the computation of MAssive TADpoles*, *Comput. Phys. Commun.* **134** (2001) 335 [hep-ph/0009029] [INSPIRE].

[50] V.A. Smirnov, *Applied asymptotic expansions in momenta and masses*, Springer Tracts Mod. Phys. volume 177, Springer, U.S.A. (2002).

[51] S. Catani and M. Seymour, *A General algorithm for calculating jet cross-sections in NLO QCD*, *Nucl. Phys.* **B 485** (1997) 291 [*Erratum ibid.* **B 510** (1998) 503-504] [hep-ph/9605323] [INSPIRE].

JHEP08(2012)139

[52] D. de Florian, G. Ferrera, M. Grazzini and D. Tommasini, *Transverse-momentum resummation: Higgs boson production at the Tevatron and the LHC*, *JHEP* **11** (2011) 064 [arXiv:1109.2109] [INSPIRE].

[53] Z. Nagy, *Next-to-leading order calculation of three jet observables in hadron hadron collision*, *Phys. Rev.* **D 68** (2003) 094002 [hep-ph/0307268] [INSPIRE].

[54] Z. Nagy and Z. Trócsányi, *Next-to-leading order calculation of four jet observables in electron positron annihilation*, *Phys. Rev.* **D 59** (1999) 014020 [*Erratum ibid.* **D 62** (2000) 099902] [hep-ph/9806317] [INSPIRE].

[55] S. Alekhin, J. Blümlein, P. Jimenez-Delgado, S. Moch and E. Reya, *NNLO benchmarks for gauge and Higgs boson production at TeV hadron colliders*, *Phys. Lett.* **B 697** (2011) 127 [arXiv:1011.6259] [INSPIRE].

[56] R. Thorne and G. Watt, *PDF dependence of Higgs cross sections at the Tevatron and LHC: response to recent criticism*, *JHEP* **08** (2011) 100 [arXiv:1106.5789] [INSPIRE].

JHEP08(2012)139